



NORTHROP GRUMMAN

DOE/ER51124-22

Final Report

**HIGH BETA AND
SECOND STABILITY REGION
TRANSPORT AND STABILITY ANALYSIS**

M.H. Hughes and M.W. Phillips.

Advanced Technology and Development Center
Northrop Grumman Corporation
4 Independence Way
Princeton, N.J. 08540

Prepared for
Department of Energy
Office of Energy Research
Acquisition Management Division, ER-64
Washington, D. C. 20545

DOE Grant No. DE FG02-89ER51124

January 1996

NOTICE

This report was prepared as an account of work sponsored by the United States Government. Neither the United States nor the Department of Energy, nor any of their employees, nor any of their contractors, subcontractors, or their employees, makes any warranty, express or implied, or assumes any legal liability or responsibility for the accuracy, completeness or usefulness of any information, apparatus, product or process disclosed or represents that its use would not infringe privately-owned rights.

MASTER

DISTRIBUTION OF THIS DOCUMENT IS UNLIMITED

DISCLAIMER

This report was prepared as an account of work sponsored by an agency of the United States Government. Neither the United States Government nor any agency thereof, nor any of their employees, makes any warranty, express or implied, or assumes any legal liability or responsibility for the accuracy, completeness, or usefulness of any information, apparatus, product, or process disclosed, or represents that its use would not infringe privately owned rights. Reference herein to any specific commercial product, process, or service by trade name, trademark, manufacturer, or otherwise does not necessarily constitute or imply its endorsement, recommendation, or favoring by the United States Government or any agency thereof. The views and opinions of authors expressed herein do not necessarily state or reflect those of the United States Government or any agency thereof.

DISCLAIMER

**Portions of this document may be illegible
electronic image products. Images are
produced from the best available original
document.**

ABSTRACT

This report describes MHD equilibrium and stability studies carried out at Northrop Grumman's Advanced Technology and Development Center during the period March 1 to December 31, 1995. Significant progress is reported in both ideal and resistive MHD modeling of TFTR plasmas. Specifically, attention is concentrated on analysis of 'Advanced Tokamak' experiments at TFTR involving plasmas in which the q -profiles were non-monotonic.

CONTENTS

I INTRODUCTION	1
1.1 Acknowledgments.....	2
II IDEAL MHD ANALYSIS OF REVERSED SHEAR EQUILIBRIA.....	3
2.1 Computational Model.....	4
2.2 Ideal MHD Stability Studies	9
2.3 Discussion of ideal MHD analysis	15
2.4 The Effects of Anisotropic Pressure on Reverse Shear Stability	16
III RESISTIVE MHD ANALYSIS OF REVERSED SHEAR EQUILIBRIA.....	20
3.1 Resistive Stability	20
3.2 Summary of Resistive MHD Stability Studies.....	24
APPENDIX	
Associated Presentations and Publications.....	26

I INTRODUCTION

This report describes work carried out at the Northrop Grumman Advanced Technology and Development Center during the period March 1st to December 31st, 1995, and supported by the Department of Energy Grant #DE-FG02-89ER51124. The work described here fulfills the program of our Research Plan for 1995, submitted during September 1994. That Research Plan emphasized theoretical and computational support for the continuing operation of TFTR during 1995. The intention of our research plan was to offer assistance in interpreting the MHD equilibrium and stability properties of experimental data from TFTR plasmas. Specifically, the program of work which we proposed was divided among two tasks as follows:

Task 1: Transport Studies and MHD Analysis of Evolving TFTR Equilibria

Task 2: Resistive MHD Modeling of TFTR Plasmas

Substantial progress is reported in each of the above topics. In particular, we have concentrated attention on recent experiments on TFTR where plasmas with non-monotonic q-profiles have been studied experimentally. These have proved interesting both from confinement physics and MHD stability points of view. It has been demonstrated in TFTR (and elsewhere) that such 'reversed shear' configurations can result in significantly improved confinement. Here, we shall discuss the MHD stability of such profiles where studies of both ideal and resistive MHD studies are described. We note that part of the work discussed here was described in two papers presented at the 1994 International Sherwood Meeting held in Incline Village, NV. and two more papers were presented at the 1995 APS, Division of Plasma Physics Meeting held in Louisville, KY during November 1995. This work was also presented in two papers at the Workshop on MHD in Reversed Shear Plasmas held at Princeton Plasma Physics Laboratory, December 14-15, 1995. A journal article describing our analysis of 'reversed shear' plasmas has been submitted for publication. These papers are enumerated in the Appendix to this document.

1.1 Acknowledgments

It is a pleasure to acknowledge the continuing interest and cooperation of numerous colleagues at TFTR and the Theory Division at Princeton, Plasma Physics Laboratory. As in previous years, we continue to maintain and expand our interaction with various other plasma physics groups throughout the country. Their informal input to our work is also acknowledged.

II IDEAL MHD ANALYSIS OF REVERSED SHEAR EQUILIBRIA

Recently, there has been renewed interest in a mode of tokamak operation characterized by non-monotonic q profiles. This interest has been motivated by recent experimental results, theoretical calculations and progress in tokamak design studies. Initially, interest in reverse shear-profiles in tokamaks resulted from the recognition that very small or even reversed shear permits access to the second stable region for ballooning modes. This allows the pressure profile to be strongly peaked in the center maximizing the achievable beta. Both DIII-D¹ and JET² have demonstrated experimentally that plasmas with reversed shear q -profiles could be produced and sustained for a significant length of time at high temperature (the q -profile evolves, however). In addition, results from these experiments suggested that such a mode of operation could lead to significantly enhanced confinement. Further interest in reversed shear plasmas was sparked during the design of the TPX tokamak³ which was intended as a steady state machine. A steady state tokamak where the diffusion driven (bootstrap) current drives most of the plasma current is a desirable configuration since it relaxes the requirements for external current drive systems and recirculating power. The current distribution resulting from the bootstrap current would naturally generate a reversed shear q profile. Theoretical studies of such configurations have found them to be as robust, from an MHD stability standpoint, as the more conventional monotonic current profiles.

The interest in reversed shear plasmas prompted an experimental study of this mode of operation in TFTR. Their results have shown that reversed shear q -profiles can lead to a new mode of enhanced confinement characterized by very low particle transport. A characteristic feature of the experiments is that a hollow current profile is generated with highly reversed shear distribution which subsequently relaxes on a resistive diffusion timescale. Both the minimum value of q and the degree of shear reversal, $\Delta q = q_0 - q_{\min}$, decrease during the course of the experiment. When q_{\min} drops to a value, $q_{\min} \sim 2$, a hard stability limit, caused by a low- n MHD mode, is encountered when beta is sufficiently large. Characterizing this stability limit is the motivation for the present study. The purpose of this study is to parameterize the stability limits resulting from low- n ($n = 1, 2$

¹ E. A. Lazarus et al., Phys. Fluids B **3**, 2220 (1991).

² M. Hugon et al., Nucl. Fusion **32**, 33 (1992).

³ C. Kessel, J. Manickam, G. Rewoldt, and W. M. Tang, Phys. Rev. Lett. **72**, 1212 (1994).

and 3) magnetohydrodynamic modes in reverse shear TFTR plasmas. An important advance, which improves the quality of MHD stability analysis of the experiments, is the development of the Motional Stark Effect (MSE)^{4,5} diagnostic for measuring the pitch of the magnetic field. The corresponding q profile can then be derived from the measurements reducing the large uncertainty involved in comparing stability computations with experimental observation. We have made extensive use of MSE data from TFTR in the present studies. Some uncertainty persists, however, since in TFTR plasmas the non-thermal beam particles contribute significantly to the pressure. This contribution to the pressure is not measured directly but obtained computationally using the TRANSP transport analysis code.

2.1 Computational Model

Here we shall confine our interest to those equilibria characterized by q profiles with a single minimum occurring at some location between the magnetic axis and plasma edge. For these profiles a region of shear reversal occurs in the central region of the plasma. The essential parameters characterizing the q profile are the value q_0 on axis, the minimum value q_{\min} , the radial location of the minimum surface and the value q_{edge} at the plasma surface. It is of interest to systematically study the effect of each of these parameters when varied independently. This demands a carefully defined procedure for prescribing the q profile when calculating MHD equilibria. Difficulties are usually encountered in parametric stability studies where q is prescribed. The steady state equilibria derived from experimental measurements are such that the current density is small or zero at the plasma edge. Arbitrarily chosen q profiles, however, often result in unrealistic current distributions in the vicinity of the boundary. A common remedy for this problem is to specify a form of the current profile, such as $\langle J \cdot B \rangle / \langle B \cdot \nabla \phi \rangle$ or $\langle J_\phi \rangle$, that can be tailored so that current reduces smoothly to zero at the boundary. Here $\langle \rangle$ denotes the flux surface average. A disadvantage of using current profiles in the present context, however, is the difficulty in exercising adequate control over all the parameters of interest. For example, simply changing β would cause both q_0 and q_{edge} to vary. Since we are interested here in controlling several characteristics of the q profile simultaneously this difficulty is compounded. The procedure described below, however, was found to adequately satisfy our requirements.

⁴ F.M. Levinton, et al., Phys. Rev. Lett., **63**, 2060 (1989).

⁵ S.P. Hirshman et al., Phys. Plasmas, **1**, 2277 (1994).

To circumvent the problem of specifying the q profile and current profile characteristics simultaneously, we choose a hybrid method in which the safety factor profile is prescribed but with a free parameter which controls the current density profile at the edge. This free parameter is chosen iteratively by the equilibrium code to keep the poloidal current density equal to zero at the boundary. Using conventional notation, the magnetic field is given by $\mathbf{B} = \nabla\phi \times \nabla\psi + g\nabla\phi$ where ψ is the poloidal flux function and (r, ϕ, z) represent a cylindrical coordinate system. The condition of zero poloidal current is then equivalent to specifying $g' = 0$, where the prime denotes differentiation with respect to ψ . We also choose $p' = 0$ at the edge which means that the toroidal current density, j_ϕ , also vanishes at the boundary.

Equilibria for this study were computed using the EQGRUM3 equilibrium code. This is a fixed boundary code which solves the Grad-Shafranov equation for the inverse equilibria $r(\psi, \theta)$ and $z(\psi, \theta)$. The code uses a fast multigrid solver which computes high resolution equilibria. EQGRUM3 is also capable of computing equilibria where the pressure is anisotropic. This feature was not been used for the study of reversed shear plasmas described in this section. A discussion of the effects of anisotropic pressure distributions is deferred to §2.4. The model safety profile was chosen to be as simple as possible while possessing all the features of the reversed shear profiles measured experimentally in TFTR. Thus, the q profile is specified in two parts - an inner and outer portion. The inner part specifies q from the magnetic axis to the minimum q location while the outer part prescribes q from the minimum q location to the plasma edge. The inner part is defined by,

$$q(\bar{\psi}) = q_0 + (q_{\min} - q_0) [2 - \bar{\psi} + c_0(1 - 2\bar{\psi} + \bar{\psi}^2)] \bar{\psi}$$

$$\text{where } \bar{\psi} = \frac{\psi - \psi_0}{\psi(q_{\min}) - \psi_0}$$

$$\text{and } c_0 = 1 + \frac{(q_{\text{edge}} - q_{\min})\psi(q_{\min})^2}{(q_{\min} - q_0)[1 - \psi(q_{\min})]^2} \text{ for } \psi_0 \leq \psi \leq \psi(q_{\min}).$$

The outer part is prescribed as

$$q(\bar{\psi}) = q_{\min} + (q_{\text{edge}} - q_{\min}) [(1 - \bar{\psi})\bar{\psi}^2 + \bar{\psi}^{\alpha_q}]$$

$$\text{where } \bar{\psi} = \frac{\psi - \psi(q_{\min})}{\psi_{\text{edge}} - \psi(q_{\min})} \text{ for } \psi(q_{\min}) \leq \psi \leq 1.$$

Here ψ_0 is the value of ψ on the magnetic axis, ψ_{edge} is the value of ψ on the plasma surface, and $\psi(q_{\min})$ is ψ at q_{\min} . The inner and outer profiles match q , q' and q'' at $\psi(q_{\min})$. A comparison of the model safety factor profile as defined above with an experimentally derived profile is shown in fig. 1. The value of α_q is generally found to be in the range 3.5 to 4.75. The specification of the relative poloidal flux at which q is a

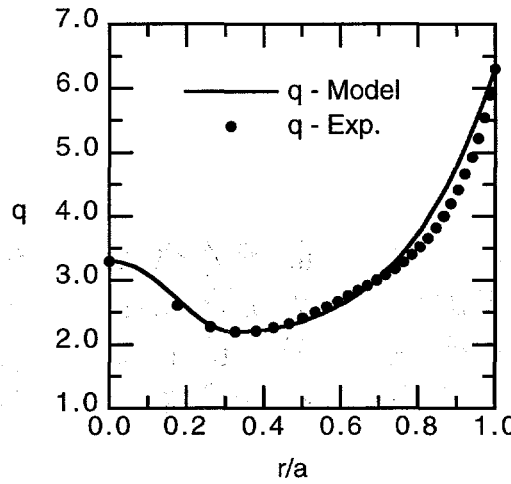


Fig 1. Model safety factor profile, q , compared to a reverse measured shear q profile in TFTR.

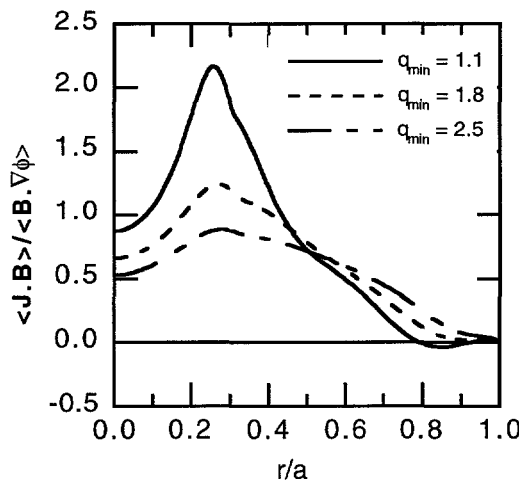


Fig. 2 $\langle J \cdot B \rangle / \langle B \cdot \nabla \phi \rangle$ profiles resulting from the model safety factor profile.

minimum means that, as q_{\min} and β vary, the radius at which q is a minimum will also vary. This change, however, is acceptably small. As an example, for a case where $q_{\text{edge}} = 6.3$, $q_0 = q_{\min} + 1$, at the marginal stability point $r_{\min}/a = 0.325$ when $q_{\min} = 1.1$. When $q_{\min} = 2.5$ then $r_{\min}/a = 0.363$. Examples of the $\langle J \cdot B \rangle / \langle B \cdot \nabla \phi \rangle$ profile resulting from this q profile specification are shown Fig. 2. As noted above, arbitrarily chosen q profiles often have unrealistic current density profiles near the edge. For example, the value of $\langle J \cdot B \rangle / \langle B \cdot \nabla \phi \rangle$ at the edge can be substantially different from zero or $\langle J \cdot B \rangle / \langle B \cdot \nabla \phi \rangle$ might even become negative. As shown in Fig. 2 the prescription for q adopted here results in $\langle J \cdot B \rangle / \langle B \cdot \nabla \phi \rangle$ being zero at the edge. For the case $q_{\min} = 1.1$ the $\langle J \cdot B \rangle / \langle B \cdot \nabla \phi \rangle$ profile has a region near the edge where it is slightly negative. Transport analysis of high current supershots usually show the $\langle J \cdot B \rangle / \langle B \cdot \nabla \phi \rangle$ to be almost zero near the outer edge of the plasma. Our prescription for specifying the q -profile models this feature adequately.

A simple formula for the pressure profile was chosen that closely models TFTR supershot pressure distributions. A typical supershot pressure profile is highly peaked on axis and decays exponentially as a function of the flux, ψ , except, possibly, near the edge of the plasma. The formula

$$p(\psi) = p_0 e^{-\alpha_1 \psi} (1 - \psi^{\alpha_2})^2,$$

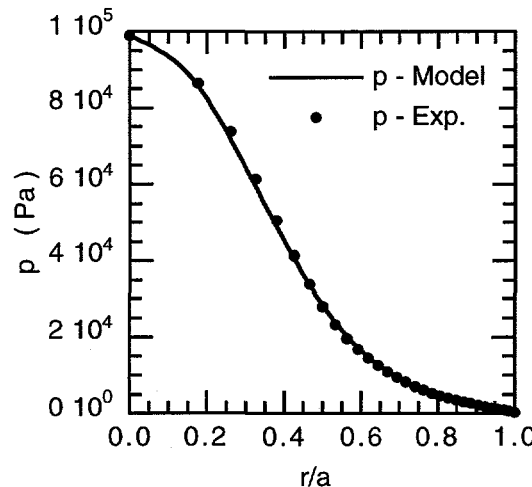


Fig. 3 Model pressure profile, p , compared with TRANSP data.

where the poloidal flux label, $\bar{\psi}$, is normalized to be zero at the magnetic axis and unity at the plasma edge, is a good representation of the TFTR data. For typical supershots the parameter α_1 lies in the range $2.5 \leq \alpha_1 < 4$. This form of the pressure profile form has two main features. First, it is an exponentially decaying function of ψ over the innermost 80% of the plasma. This usually matches supershot data very accurately. The second component of the profile forces both p and p' to tend smoothly to zero at the plasma edge. It also models a small increase in the pressure gradient near the boundary which is also a feature of the experimental data. The parameter α_2 is chosen to be large, ~ 10 . The central pressure p_0 is adjusted to change the value of β as required. A comparison with a pressure profile computed from transport analysis of an actual experiment in TFTR is illustrated in Fig. 3.

The equilibria for these studies were computed on a grid of 129 radial surfaces and 320 poloidal nodes. The estimated maximum truncation error due to the finite size grid is less than 3×10^{-4} when compared with the fully converged solution. As the limiting β for ideal MHD stability is approached from above the radial derivatives at mode rational surfaces tend to become very steep. To accurately represent this computationally in the stability codes a finer mesh than is used by the equilibrium solver. This is accomplished by mapping the equilibria to a larger number of radial surfaces using a separate mapping code.

The ideal MHD stability analysis was performed using the KOSMIK low-n stability code. This code was originally designed to compute the low n-number Kruskal-Oberman stability. For computations described here, the code was adapted to solve the isotropic, incompressible MHD equations. In this version of the code the MHD equations are written in terms of a vector stream function, \mathbf{u} such that $\mathbf{v} = \nabla \times \mathbf{u}$ where \mathbf{v} is the perturbed fluid velocity. A gauge transformation is chosen such that $u_\phi = 0$. Although this choice of gauge precludes the case where the toroidal mode number, $n = 0$, it conveniently simplifies the matching of the vacuum solution at the plasma surface. The KOSMIK code can include the vacuum region between the plasma and a conducting boundary. The code also has the capability of modeling multiple, perfectly conducting surfaces. Most of the ideal MHD computations presented here invoked a "wall at infinity" boundary condition (i.e. no external conducting surfaces) except where otherwise noted. This boundary condition generally results in the most pessimistic stability criteria. KOSMIK has been benchmarked against the ARES code¹ and several specific reverse shear cases were compared in detail using the two codes. When numerically converged both codes were found to be in satisfactory agreement.

2.2 Ideal MHD Stability Studies

The prototype for the equilibria modeled here was taken from shot #83998 at $t = 2.99$ seconds. This particular shot was chosen because it had good quality diagnostic data including MSE measurements from which the q profile was derived. It did not, however, enter the so called Enhanced Reverse Shear (ERS) mode where the particle transport is observed to be reduced by a large factor. There was MHD activity which appeared toward the end of the shot which ultimately terminated with a disruption, typical of those observed on other reversed shear shots. The geometrical parameters for the equilibria in this study are $R = 2.59$, $a = 0.92$ and $\epsilon = 1.05$. This represents a plasma which fills most of the available cross section of TFTR and is typical of reversed shear equilibria. For shot #83998 at $t = 2.99$ seconds the equilibrium had $q_{\text{edge}} = 6.3$, $q_0 = 3.2$ and $q_{\text{min}} = 2.2$ with the minimum located at $\psi(q_{\text{min}}) = 0.15$. The corresponding pressure profile parameters were $\alpha_1 = 4$, and $\alpha_2 = 20$.

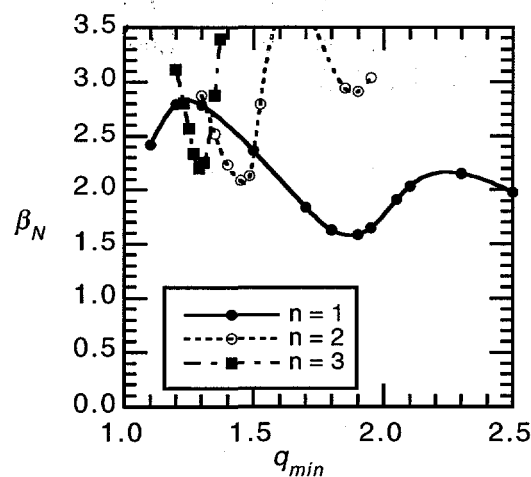


Fig. 4. Normalized beta limits of low- n instabilities as a function of the minimum q value. For these cases $q_{\text{edge}} = 6.3$, $\Delta q = q_0 - q_{\text{min}} = 1.0$, $\alpha_p = 4$.

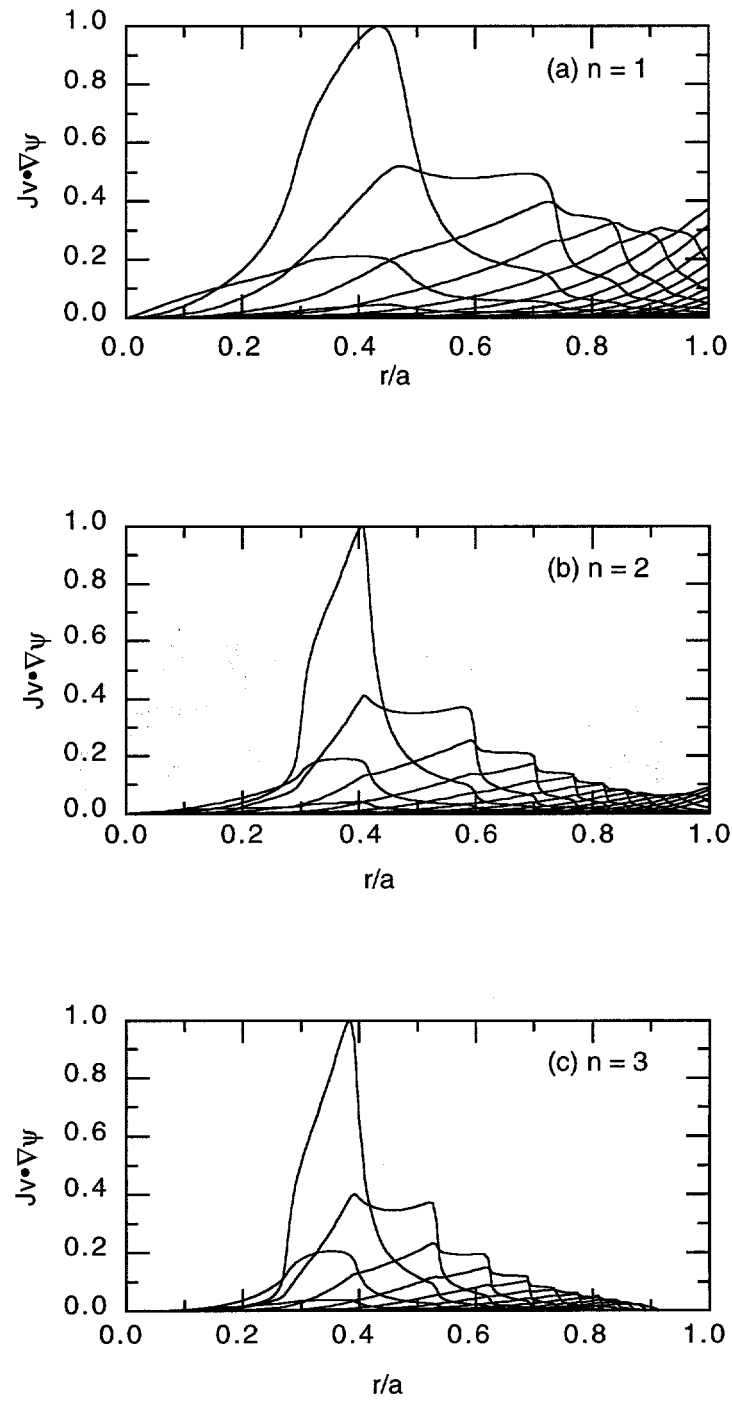


Fig. 5. Radial component of the perturbed velocity for a) $n = 1$, b) $n = 2$, c) $n = 3$ for the mode with the lowest beta limit.

Typically, q_{\min} decreases during the course of the experiment until it reaches a value ~ 2.0 when a low n instability appears. To gauge the effect of q_{\min} on the beta limit, this parameter was varied and the critical beta for marginal stability was computed for each of the $n = 1, 2$ and 3 modes. The result is shown in Fig. 4 which plots the normalized beta, $\beta_N = \beta / (I/aB)$, as a function of q_{\min} . For this calculation the difference between the central and minimum values of q value, Δq , was kept fixed at 1 (i.e. $\Delta q = q_0 - q_{\min} = 1$). The location of the minimum q value, $\psi(q_{\min})$, and q_{edge} were held fixed in these calculations. Also, the 'wall at infinity' boundary condition was invoked. The minimum value of q was found to have an important influence on the critical beta limit. In particular, the beta limit is reduced abruptly as q_{\min} approaches rational values. For the $n = 1$ mode this feature is due to an instability where the poloidal mode number $m = 2$ is the dominant harmonic. The structure of the limiting instability becomes a purely internal mode as q_{\min} approaches a rational value, as can be seen from fig. 5. On the other hand, when $q_{\min} > 2$ the mode has a much greater 'external' component. In contrast the $n = 2$ and $n = 3$ modes have little external component and were essentially 'internal' modes. Fig. 5 shows the mode structure of the instabilities for a) $n = 1$, b) $n = 2$ and c) $n = 3$ just inside the unstable region at the point where β_N is a minimum for each mode number. The dip in β_N for the $n = 1$ mode near $q_{\min} = 2$ (fig. 4) correlates closely with the stability boundary that limits the pressure in the experiment. During the course of an experiment q_{\min} slowly decreases as current diffuses into the center of the plasma. Near $q_{\min} = 2$ instability occurs leading to disruptive loss of the plasma.

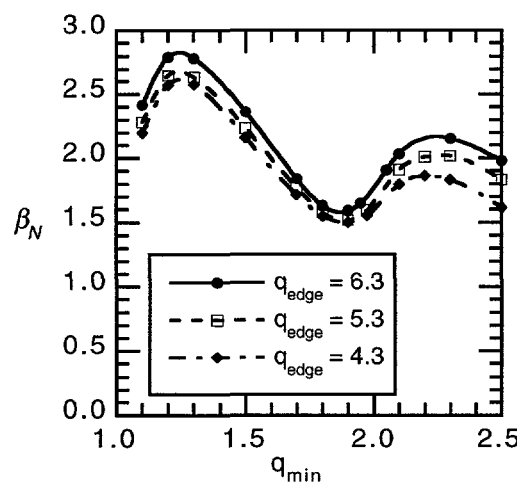


Fig. 6. The normalized beta limits for the $n = 1$ instability as a function of the minimum q value for different q_{edge} values.

The effect of changing the value of q at the surface of the plasma, q_{edge} , and hence the total current, is illustrated in Fig 6 for the $n = 1$ mode. The essential features of the stability diagram, namely the lower beta limits near rational values of q_{min} , remain the same. Indeed, this feature is typical of all reversed shear equilibria. As shown in Fig 6, when the plasma current increases the normalized beta decreases only slightly below $q_{\text{min}} = 2$. The beta limit appears to be a beta-normal limit. Above $q_{\text{min}} = 2$ the difference is somewhat larger. This is due to the broadening of the current profile which tends to decrease the stability limit for external modes. The current profile is broadened both by the decrease in q_{edge} and the increasing q_{min} which redistributes the current to the outside. For $q_{\text{min}} > 2$ the mode is a mixture of an infernal mode and an external kink mode.

The form of the pressure distribution also has a significant effect on the stability of the infernal mode. Fig 7 shows the $n = 1$ stability boundaries as the pressure distribution is broadened. Typically pressure profiles in TFTR tend to be quite peaked. As the pressure

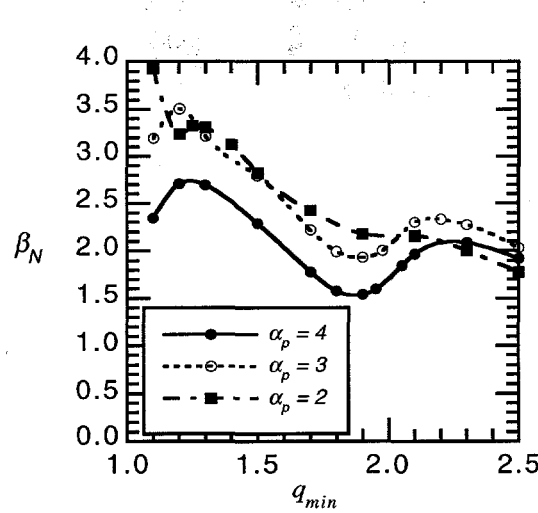


Fig. 7 The effect of pressure profile peaking on the normalized beta limits for the $n = 1$ instability as a function of the minimum q .

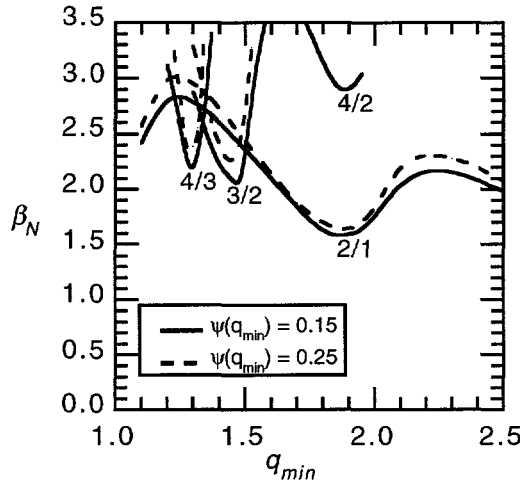


Fig. 8. The effect of shear reversal radius on the normalized beta limits for the $n = 1$ instability as a function of the minimum q .

distribution broadens the maximum normalized beta increases. There appears to be a limit, however, to how broad the pressure profile can be and still achieve this effect. There is little overall increase in the beta limit for the case $\alpha_p = 2$ when compared to $\alpha_p = 3$. Indeed, for the $\alpha_p = 2$ case the nature of the instability that limits beta changes, becoming more an external kink mode with the effect of the resonance at $q_{\min} = 2$ barely detectable.

So far the stability of reversed shear profiles is similar, in many respects, to previous studies of supershots with monotonic q profiles⁶. In both cases the infernal mode causes a decrease in the beta limit when q_{\min} (or the central value $q(0)$ in the case of monotonic profiles) is near a rational value. One difference is that the beta limit due to higher n number modes ($n \geq 2$) is now higher than that computed for monotonic profiles. Starting with a monotonic q -profile with low central shear the beta limit increases as the central shear increases until a peak is reached and the beta limit subsequently decreases. The question is whether the beta limit continues to decrease when central shear is reversed. The two parameters of interest are the location of minimum shear $\psi(q_{\min})$ and $\Delta q = q_0 - q_{\min}$. The first parameter determines the radial extent of the reversed shear region and the second parameter is a measure of the degree of shear reversal. Fig 8 demonstrates the result of shifting the radial location of the minimum in q to larger radii. Overall the effect tends to be stabilizing. The minimum beta limit associated with the mode rational surfaces tends to

⁶M. H. Hughes, M. W. Phillips, E. D. Fredrickson, Phys. Fluids B 5, 3267 (1993).

be increased for the higher n modes compared to the $n = 1$ mode. Changing $\psi(q_{\min}) = 0.15$ to $\psi(q_{\min}) = 0.25$ causes the relative minor radius to move out about 0.1. Fig. 9 shows the effect that changing $\Delta q = q_0 - q_{\min}$ has on the $n = 1, 2$ and 3 stability boundary. The stability boundaries for the cases $\Delta q = 1$ and $\Delta q = 0.1$ are shown. Increasing Δq tends to increase the normalized beta limits. As in the case of increasing the inversion radius, increasing Δq seems to have a larger effect on the $n = 2$ and 3 modes than on the $n = 1$ mode. Several cases were run to determine whether the effects are multiplicative. Increasing both Δq and shear reversal radius leads to proportionally higher beta limits.

Fig. 9

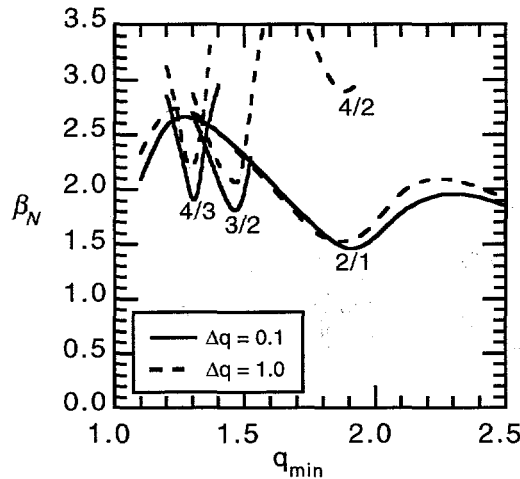


Fig. 9. The effect of shear depth on the normalized beta limits for the $n = 1$ instability as a function of the minimum q .

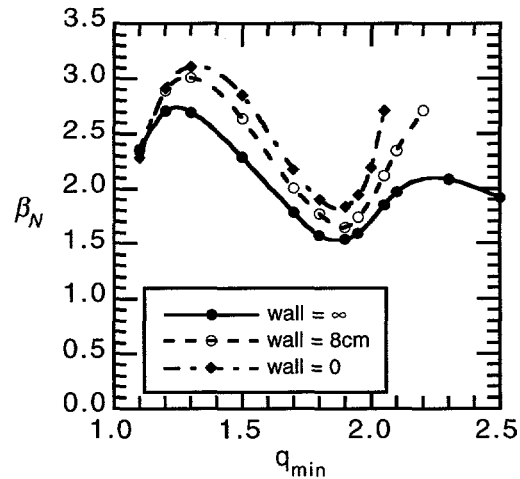


Fig. 10. The effect of perfectly conducting wall radius on the normalized beta limits for the $n = 1$ instability as a function of the minimum q .

So far we have considered only cases where there was no stabilization due to a conducting wall surrounding the plasma. Fig.10 shows the effect of a perfectly conducting wall surrounding the plasma. The wall was located at a constant distance from the plasma surface. As expected the wall has little effect when the mode is mainly internal as occurs when q_{\min} is near a rational value. However there is a strong stabilizing effect when $q_{\min} > 2$ where the marginally stable mode has a larger external component.

2.3 Discussion of ideal MHD analysis

Equilibria with a reversed shear region have low- n stability properties similar to those with monotonic q profiles having low central shear. In both cases the main mode of instability limiting the achievable beta is an internal mode. This stability boundary appears to correlate with that found experimentally during reversed shear experiments in TFTR. The reverse shear case differs from the monotonic q profile case in that the higher n modes ($n > 1$) are more stable. The lowest beta limit is set by the $n = 1$ mode near $q_{\min} = 2$. More reverse shear either in the form of an increased $\Delta q = q_0 - q_{\min}$ or a larger reversal radius both tend to improve the stability limits of the $n = 1, 2$ and 3 modes. A greater improvement in the beta limit occurs for the higher n modes, $n = 2$ and 3 . Thus, some shear whether it is positive or reversed seems to be beneficial to low- n stability. If rational values of q_{\min} can be avoided the beta limit for TFTR is greater than can be achieved for monotonic profiles. In the range $1 < q_{\min} < 2$ reversed shear profiles have an advantage over monotonic profiles by raising the beta limit caused by higher n modes. Another avenue for increased beta is to keep $q_{\min} > 2$. In this region the higher n modes are stable. If wall stabilization is effective in stabilizing the $n = 1$ external kink mode further gains in beta are possible.

2.4 The Effects of Anisotropic Pressure on Reverse Shear Stability

The discussion so far has concentrated exclusively on pressure profiles which were assumed isotropic. However, high β equilibria in TFTR, including those with reversed magnetic shear, typically have anisotropic pressure distributions resulting from the intense beam heating. The pressure anisotropy arises as a result of the difference in the slowing down times of the neutral beam particles in the perpendicular and parallel directions. The pressure distribution in TFTR usually has enhanced parallel pressure distribution. Generally the pressure distribution is highly anisotropic at early times when the neutral particle beams are first turned on and then becomes increasingly isotropic as the plasma

evolves. The degree of pressure anisotropy also depends sensitively on the plasma density since the rate at which the hot ions equilibrate depends on this parameter. Fig 11 shows the relative difference in the parallel and perpendicular pressure distributions as a function of time for TFTR shot #75963. This shot had a reversed shear q-profile that entered the so called ERS ('Enhanced Reversed Shear') mode characterized by improved

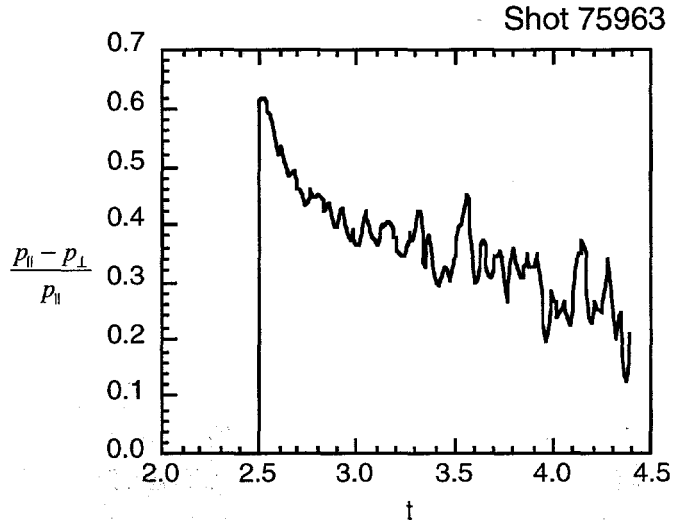


Fig 11 Relative difference in pressure components for reverse shear shot # 75963

confinement. This shot had MHD activity starting around $t = 4.3$ seconds and a disruption occurred shortly after. For supershots the degree of pressure anisotropy is typically in the range $0.15 < (p_{\parallel} - p_{\perp})/p_{\parallel} < 0.25$ with the parallel pressure dominant near the end of the discharge. For shot # 75963 $(p_{\parallel} - p_{\perp})/p_{\parallel} \sim 0.25$ at the time that MHD activity started.

In previous studies of TFTR anisotropic pressure effects did not appear to be important. This is due to a combination of factors but due mainly to the fact that TFTR has a relatively low beta with $\beta < 1\%$. The quantity $(p_{\parallel} - p_{\perp})/B^2$ is on the order of 0.0025 which is too small to influence the anisotropic pressure terms in the force balance equation. The largest effect in a low beta tokamak arises from the influence of the parallel pressure distribution on the parallel current as can be seen from the formula,

$$\frac{j_{\parallel}\sigma}{B} = -\frac{\partial G}{\partial \chi} - \frac{g}{B^2} \frac{\partial p_{\parallel}}{\partial \chi} \bigg|_B .$$

A series of computations were performed to determine the effect, if any that, anisotropic pressure distributions have on the stability characteristics of reversed shear TFTR equilibria. A version of the KOSMIK low-n code that implements the anisotropic

stability problem was used. As mentioned in §2.1 the code is based on the Kruskal Oberman energy principle. It does not, however, include the effect of adiabatic compressibility that is part of that formalism. The adiabatic compressibility term is positive definite and stabilizing but is somewhat difficult to compute since it involves integrals over the pitch angle. This term is similar in order to the MHD compressibility term. It differs from ideal MHD in that it does make a difference in the marginal stability point. Previous computations on ballooning modes which included this term showed its effect on the marginally stability point to be quite small, even at high beta. For these initial computations it was our intention to estimate the magnitude of anisotropic pressure effects. Therefore, we initially neglected the adiabatic compressibility term. Fig 12 shows the evolution of β in TFTR shot # 75963 as a function of time. Also depicted are the beta limits for the isotropic case, for the case where the parallel pressure dominates and for a third case where the perpendicular pressure was dominant. The beta limit was determined for three equilibria taken from the TRANSP simulation of this run. To determine the beta limit the q profile was held fixed and the pressure distribution was scaled by a constant. In all cases the limiting instability was an infernal mode. As can be seen from Fig 2 pressure distributions where the parallel pressure is largest are mildly destabilizing while pressure distributions with perpendicular anisotropy are stabilizing. Overall, the effect is noticeable but not significant.

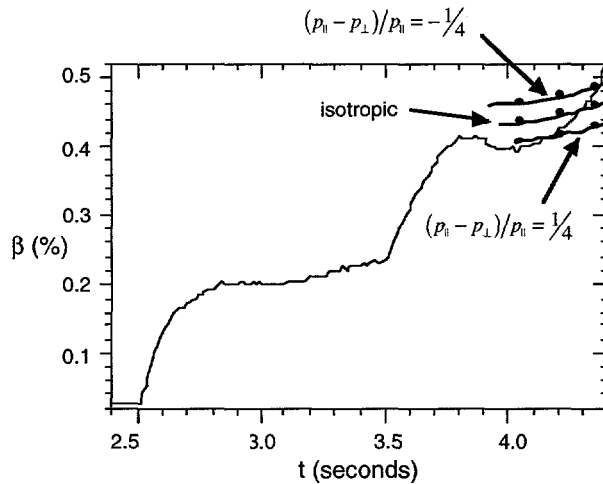


Fig 12 Beta as a function of time shot # 75963 and computed $n = 1$ stability limits for isotropic and anisotropic pressure distributions.

The effect of an anisotropic pressure distributions on ballooning stability was also evaluated. A version of the STBAL code that includes anisotropic effects in the ballooning and Mercier stability was used. A novel feature of this code is that the effect of the perturbed anisotropic equilibria on ballooning is including allowing both the first and

second regions of stability to be mapped out. Fig.13 shows the ballooning stability of shot # 75963 at $t = 4.21$. This is just before the observation of MHD activity in this shot. It is evident from Fig.13 that an anisotropic pressure distribution has very little effect on the ballooning stability. Interestingly, and characteristic of ERS shots, is that the central pressure gradient reaches well into the second region of stability.

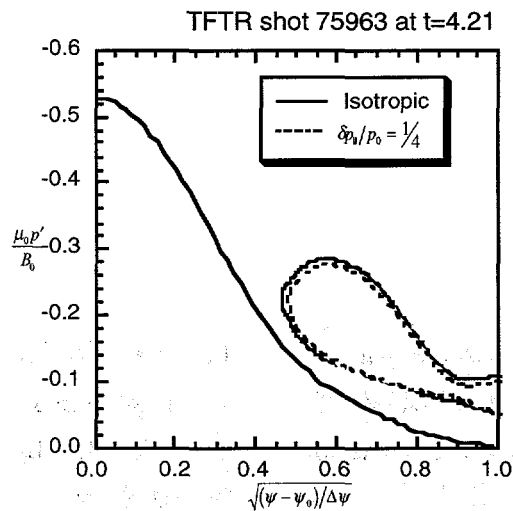


Fig 13 Ballooning beta at $t = 4.21$ sec. for shot # 75963 for isotropic and anisotropic pressure distributions.

In summary, reverse shear shots tend to have pressure distributions where the parallel pressure dominates. Inclusion of the effects of anisotropy on stability tends to lower beta limits for the $n = 1$ mode. The effect is small due to the low beta in the device. The effect of anisotropic pressure distributions on ballooning instability was also computed for this shot and was also found to be even smaller.

III RESISTIVE MHD ANALYSIS OF REVERSED SHEAR EQUILIBRIA

The previous section described in detail the ideal (infinite conductivity) stability analysis of 'reversed shear' plasmas produced in TFTR. Here, those studies are extended to include the effect of finite plasma conductivity and to consider the possible role of resistive instabilities in these experiments. In plasmas where the current density distribution has an off-axis maximum there can be two resonant surfaces for a mode with given m/n . It is then possible to excite 'double tearing' modes producing magnetic islands which can grow at each surface with a poloidal phase difference between the two sets of islands. It has long been believed that such instabilities may contribute to the rapid penetration of the plasma current during the startup phase of a tokamak. The nonlinear evolution of the double tearing mode is of particular interest since these modes can either saturate or, alternatively, result in magnetic reconnection with disruptive changes to the safety factor profile⁷ in a manner reminiscent of the 1/1 sawtooth instability. Indeed, there is a suggestion that multiple tearing modes at rational surfaces can, with some differential rotation, grow explosively⁸. An interesting experimental observation from TFTR, however, is that their high temperature plasmas with non-monotonic safety factor profiles typically evolve without coherent MHD activity until such time that they encounter the ideal MHD β -limit.

3.1 Resistive Stability

The procedure adopted here for calculating equilibria where the safety factor has an off-axis minimum is identical with that used for the ideal MHD studies. That is, the pressure profiles are obtained from TRANSP analysis of the experiments and simply scaled to alter β while a model procedure for is used to prescribe q . The q -profiles are, however, in reasonable accord with those derived experimentally from MSE measurements of the pitch of the magnetic field. This method (described in detail in §2.1) allows us to vary the parameters describing the reversed shear profiles in a systematic fashion and to calculate subsequent changes to the stability properties of the system. Here, we concentrate on plasmas where both the location of the minimum in q and the edge value of the safety factor, $q_e = 6.3$, are fixed. The minimum value, q_{\min} , of q is varied keeping the central value, $q(0) = q_{\min} + 1$. These parameters, similar to the values used in §2.1, are chosen

⁷ Carreras, B., Hicks, H.R. and Waddell, B.V., Nuc. Fusion, **19**, (1979), 583 - 596.

⁸ Persson, M., Phys. Fluids B, **5**, (1993), 3844-3846.

to model a typical reversed shear, TFTR equilibrium. The resistive stability of these equilibria was subsequently analyzed using a linear version of the ARES code. Initial studies of the nonlinear evolution of the resistive double tearing modes are currently in progress. We also note in passing that, when the resistivity is set to zero the ARES and ideal MHD, KOSMIK, codes used in these studies yield results in agreement to within $\sim 1\%$.

Using the results from the ideal MHD calculations as a guide, we have studied the excitation of resistive instabilities in regions of parameter space where the ideal modes are stable. Note that, all these resistive MHD calculations invoke a boundary condition of a perfectly conducting wall in contact with the plasma periphery (unlike the discussion of §2.3 where it is assumed that there is a vacuum region between the plasma and a perfectly conducting wall). The main result of these linear calculations is that there is a wealth of purely resistive MHD modes that appear at all pressures from zero to the ideal MHD limit. For example, fig. 11 displays the growth rates of the resistive instabilities as a function of the minimum value, of q at fixed $\beta = 0.72\%$ and fixed Lundquist number (magnetic Reynolds number), $S = 10^7$. This value of β is chosen to be near, but on the stable side of the boundary for the most unstable ideal mode; that is, the mode with toroidal mode number, $n=1$, at $q_{\min} = 1.85$ (see fig. 10, §2.2). Note from fig 14 that as q_{\min}

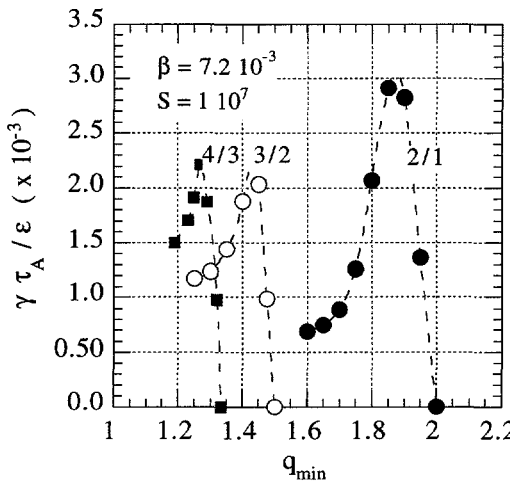


Fig. 14 Resistive Mode Growth Rates as q_{\min} is Varied

is reduced from large values (> 2) there is a sudden onset of instability with mode numbers $m/n = 2/1$ as q_{\min} passes through 2. As q_{\min} continues to decrease the growth rate of the $2/1$ mode quickly attains a maximum and then decreases rapidly until a $3/2$

instability appears when $q_{\min} < 1.5$; subsequently a 4/3 mode is excited as q_{\min} continues to decrease and presumably higher order m/n modes would appear at even smaller values of q_{\min} . Note that, the maximum growth rates shown in this diagram have significant magnitudes. For example, $\gamma \tau_A / \epsilon = 10^{-3}$ corresponds roughly to a growth time of $100\mu\text{sec}$, assuming typical TFTR parameters.

Interestingly, the general behavior illustrated in fig 14 persists at all pressures from zero to the marginal stability boundary for ideal modes. Fig.15 shows the variation of the growth rate of the 3/2 mode as the pressure is varied at fixed q_{\min} and fixed S . In these calculations there is no significant stabilization of the instability due to finite pressure effects⁹ even though $\beta_p > 1$ at the highest pressures of interest. Fig. 15 shows that there is only a modest reduction in the growth rate as the pressure is initially increased from zero but as the pressure continues to increase the growth rate passes through a minimum and subsequently increases significantly as the ideal MHD boundary is approached.

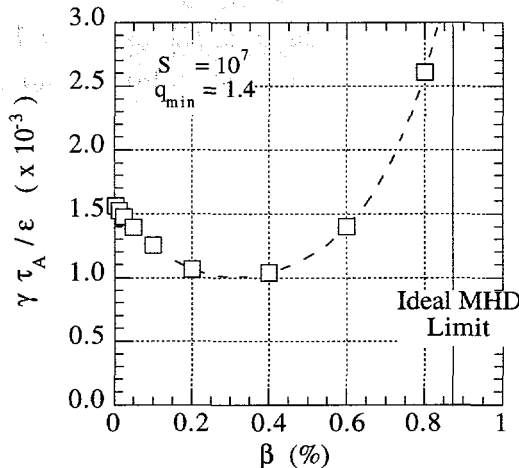


Fig. 15 Variation of $n=2$ Resistive Mode Growth Rates with Plasma Pressure

The apparent absence of significant pressure stabilization of the resistive (tearing) modes is due to the fact that the character of the instability changes as we traverse the curve shown in fig 15. Tearing modes or double tearing modes appear only when the plasma parameters are well away from the ideal MHD stability limit. Indeed, analytic theory

⁹ Iacono, R., Bhattacharjee, A., Ronchi, C., Greene, J.M. and Hughes, M.H., Physics of Plasmas, **8**, (1994), 2645.

predicts¹⁰ that when the pressure (or any other appropriate parameter) approaches the marginal value for ideal MHD instability from the unstable side the instability becomes a resistive mode with a growth rate scaling as $S^{-1/3}$. As the pressure (or other parameter) continues to change the mode eventually becomes a tearing mode scaling as $S^{-3/5}$. This behavior is confirmed computationally and is illustrated in fig. 16. This graph plots the resistive mode growth rates of the $n=2$ mode as functions of the Lundquist number at different pressures. The largest value of the pressure in this case corresponds to the marginal ideal point for the $n=2$ instability, found using the KOSMIC code.

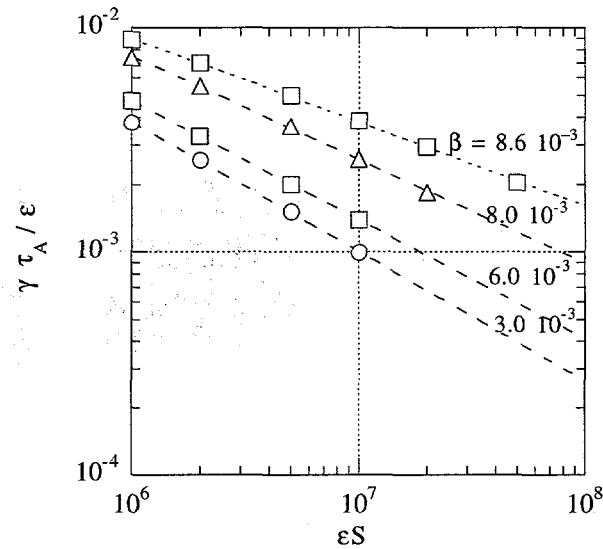


Fig. 16 Variation of the Resistive Mode Growth Rates with the Lundquist Number. This graph illustrates how the exponent of S changes from $1/3$ at the ideal marginal stability point to $3/5$ as the pressure (in this case) is sufficiently reduced.

Thus, the tearing modes appear only when the pressure is substantially smaller than the limiting value determined by ideal MHD. Note that this statement also holds in the case of fig.14 where q_{\min} is the independent variable. In this case, the pressure was deliberately chosen to correspond to the minimum value of β_N set by the 2/1 mode (fig. 10, §2.2) but much smaller than the limiting value for higher m/n modes. Thus, the character of the mode also changes with q_{\min} in fig. 14. We find that, the 2/1 mode exhibits the $S^{-1/3}$ scaling of the growth rate since β is near the ideal stability limit for this mode. In

¹⁰ Coppi, B., Galvao, R.M.O., Pellat, R., Rosenbluth, M.N. and Rutherford, P.H., MATT-1271, Princeton Plasma Physics Laboratory

contrast, the higher m/n modes display the $S^{-3/5}$ (tearing) variation since, for these modes, β is well below the marginal point for ideal MHD instability.

A further qualitative observation regarding the tearing mode regime is as follows. As q_{\min} passes through a rational value from above the two surfaces of interest are initially very close (the degenerate case is of no interest). The two tearing layers can then be coupled resulting in the 'double tearing' configuration that is found computationally. As q_{\min} decreases further the procedure adopted here for altering q causes the two rational surfaces to move further apart in radius and with respect to the current density profile. The coupling of the two resonant surfaces then becomes weaker until a point is reached where the two surfaces no longer interact. The mode then becomes a 'regular' tearing instability centered at the innermost rational surface. These tearing and double tearing modes are, indeed, influenced by finite pressure effects.

The tearing type modes, with $S^{-3/5}$ scaling of the growth rates, have relatively little harmonic structure and tend to be localized in the vicinity of the appropriate rational surfaces. On the other hand, the $S^{-1/3}$ modes which appear at higher pressures have much more harmonic structure and are more 'global' in nature. That is, the perturbation extends over a large fraction of the radius and are, therefore, probably more damaging. It is unlikely that the experiment can distinguish these latter instabilities from the ideal MHD modes which occur at slightly higher pressure. At the present time, $q_{\min} \sim 2$ is the smallest value achieved in TFTR before the ideal $n=1$ mode is excited and the plasma disrupts. The resistive modes which are predicted to appear could well pose a problem in attempts to operate at $q_{\min} < 2$. The tearing and double tearing modes that are excited at low pressure may, however, be stabilized by mechanisms not modeled here. Plasma rotation, which decouples the resonant surfaces¹¹ or nonlinear saturation of the mode, for example, are both possible candidates.

¹¹ Persson, M., Physics of Plasmas, **1**, (1994), 1256-1263.

3.2 Summary of Resistive MHD Stability Studies

In summary, the main conclusions of the section on resistive MHD are as follows:

- Resistive instabilities are predicted by MHD theory at all pressures from zero to the infinite conductivity limit in the reversed shear plasmas studied for TFTR plasmas with $q_{\min} < 2$.
- The double tearing mode, thought to contribute to the rapid penetration of current when the q profile has an off-axis minimum, appears only at low pressure. In the vicinity of the ideal MHD limit there is an $S^{-1/3}$ resistive mode.
- TFTR operation with $q_{\min} < 2$ might be impaired by the excitation of resistive tearing and double tearing modes.

APPENDIX: Associated Presentations and Publications

1. M.H. Hughes and M.W. Phillips, *MHD Stability of Reversed Shear Current Profiles*, 1995 International Sherwood Fusion Theory Conference, Incline Village, Nevada, April 1995, Paper 2D28
2. M.W. Phillips and M.H. Hughes, *MHD Stability of Advanced Operating Regimes in Tokamaks*, 1995 International Sherwood Fusion Theory Conference, Incline Village, Nevada, April 1995, Paper 2D30
3. M.H. Hughes and M.W. Phillips, *MHD Stability of Reversed Shear Current Profiles*, 37th Annual Meeting, APS Division of Plasma Physics, Louisville, KY, 1995
4. M.W. Phillips and M.H. Hughes, *MHD Stability Issues of Advanced Tokamak Concepts*, 37th Annual Meeting, APS Division of Plasma Physics, Louisville, KY, 1995
5. M.W. Phillips, *A Parametric Survey of Ideal Stability Limits of Reversed Shear Equilibria*, Workshop on MHD in Reversed Shear Plasmas, Princeton Plasma Physics Laboratory, December 14-15, 1995
6. M.H. Hughes and M.W. Phillips, *Resistive MHD Studies of Reversed Shear, TFTR Plasmas*, Workshop on MHD in Reversed Shear Plasmas, Princeton Plasma Physics Laboratory, December 14-15, 1995
7. M.W. Phillips, M.H. Hughes, F. Levinton, J. Manickam and M. Zarnstorff, *Low- n Magnetohydrodynamic Stability Studies of Reversed Shear Equilibria in TFTR*, submitted to Physics of Plasmas.